The promotion of nickel to Mo_2C/Al_2O_3 catalyst for the partial oxidation of methane to syngas

Zhu Quanli, Zhang Bing, Yang Jian, Wang Jiaxin, Zhao Jun, Ji Shengfu* and Wang Hanqing*

State Key Laboratory for Oxo Synthesis and Selective Oxidation, Lanzhou Institute of Chemical Physics, Chinese Academy of Sciences, Lanzhou 730000, P. R. China.
E-mail: qlzhu0001@sina.com.; Fax: +86-931-8277088; Tel: +86-0931-8278319

Received (in Cambridge, UK) 9th June 2003, Accepted 31st July 2003
First published as an Advance Article on the web 4th September 2003

Alumina-supported molybdenum carbide and its modifier with small amounts of nickel were evaluated and characterized. The evaluation results showed that a nickel-doped carbide catalyst exhibited a much higher conversion of methane and selectivity to CO and $H_2$for the partial oxidation of methane (POM) to syngas. Also, the addition of a small amount of nickel resulted in significant improvement of catalysis stability. Characterization by temperature programmed surface reaction (TPSR) indicated that the addition of nickel promoted the carburization of molybdenum oxide. Especially under the conditions of the POM to syngas, this promotion resulted in more active phases being held. The nickel doped catalyst had small particles, larger specific area and greater ability to resist sintering. All these improved the catalytic stability. The other characterizations by XRD, XPS, SEM as well as BET surface area measurement also confirmed these promotions of nickel. In addition, the doped nickel made possible the increase of the intrinsic activity of catalytic centers over molybdenum carbide catalyst.

1. Introduction

Carbides, particularly of transition metals, have a number of valuable properties, such as high melting temperature, extreme hardness, abrasion resistance and inert chemical activity at room temperature, *etc.* which makes them the most promising materials for use in the fields of new technologies. They have been used in cutting tools, mining tools and machine tools *etc.*[1–4] A number of attempts have focused on exploiting their catalytic properties since it was reported by Levy and Boudart[5] that there was a similarity between tungsten carbide and noble metal catalysts. Transition metal carbides, in particular molybdenum and tungsten carbides, exhibited excellent catalysis similar to group VIII B transition metals in the periodic table in the reactions including hydrodenitrogenation (HDN) and hydrodesulfurization (HDS),[6–15] isomerization of hydrocarbon,[16–20] hydrogenation of carbon oxide and Fischer–Tropsch synthesis,[21–23] as well as electrocatalytic reactions over the electrodes of fuel cells.[24,25] These reactions are commonly involved in H-transfer reactions.

Recently, an investigation into the performance of molybdenum and tungsten carbides for the partial oxidation of methane (POM) to syngas was performed by Green and coworkers.[26–28] It was found that molybdenum carbide had an activity similar to iridium both per active site and per gram under the stoichiometric conditions and elevated pressure, and no deposited carbon was observed on the post-reaction samples.[26–28] However, it deactivated rapidly at ambient pressure. They ascribed the deactivation of the catalyst mainly to the oxidation of carbide into oxide, followed by vaporisation of molybdenum oxide. This deactivation could be improved when supported, although only to some extent. If the catalyst was deactivated in that way, there was a resistance to the transformation of oxide into carbide during the POM to syngas. If so, it can facilitate carburization of metal oxide. The catalyst can be further prevented from deactivation under the reaction conditions, if some material, capable of producing carbon active enough to replace oxygen in oxide, is added. Based on this hypothesis, the addition of a range of metal oxides was investigated, and among them, a small amount of nickel oxide was shown to significantly improve the activity and stability of molybdenum carbide catalyst. Thus the investigation on the roles of nickel in Mo_2C/Al_2O_3 catalyst made up our contribution.

2. Experimental

2.1 Catalyst preparation

According to our activity evaluation results of Mo_2C/Al_2O_3 catalysts with different loading, sample 50 wt.% MoO_3/Al_2O_3 (whose corresponding carbide exhibited better catalytic performance) was chosen as the oxide precursor. It was prepared using an impregnation method. In brief, the calculated amount of γ-alumina (BET surface area, 303 $m^2\ g^{-1}$) was impregnated with the ammonia solution containing a calculated amount of ammonium heptamolybdate (A.R.) or the mixed solution of a calculated amount of ammonium heptamolybdate and nickel nitrate (A.R.) at room temperature for 4 h, then the mixed solution was evaporated to dryness with stirring in a water bath at *ca.* 358 K. The obtained powder was transferred into an oven with temperature controlled and held at 115 °C for 12 h. Finally, it was calcined in air at 773 K for 4 h. Thus, the oxide precursor was obtained. Ni/Al_2O_3 was prepared using alumina impregnated with the calculated amount of nickel nitrate solution. Other procedures were same as the above.

The carburization of precursor was carried out according to a temperature programmed reaction (TPR) method.[29,30] The oxide precursor (usually 0.15 g) loaded in a quartz tube (4 mm id) was carburized using 20 vol.% of flowing methane (nominal purity, 99.99%) in hydrogen (nominal purity, 99.99%) at a total flow rate of 35 ml min^{-1}, heated at a ramped rate of 10 K min^{-1} from room temperature to 573 K, and then

at 1 K min^{-1} from 573 to 1123 K, finally, maintained at 1123 K for 2 h. The tube furnace was controlled by a PID controller with accuracy of ±1 K. After it was pretreated with H_2 (28 ml min^{-1}) for half an hour, the prepared nickel-doped carbide catalyst was either evaluated *in situ* or cooled in helium (nominal purity, 99.99%) to room temperature and then passivated with 1 vol.% O_2 (nominal purity, 99.9%) in helium (20 ml min^{-1}) at room temperature for 12 h for the purpose of characterization.

2.2 Catalyst testing

Catalysts were *in situ* evaluated just after carburization and pretreatment with hydrogen in a continuous flow fix bed reactor at ambient pressure using a mixture of methane and oxygen as feedstock. Reactant gases were controlled with a mass controller. The gas mixture, when it became stable, was switched to the quartz tube equipped with coarse quartz wool plugged in the central part to uphold samples. The thermocouple was placed at the outer reactor close to the catalyst bed. The products were analyzed online by chromatography (SC-8 Model, Sichuan Analysis Apparatus Machinery, P.R. China) with 5A zeolite and Porapak Q packed columns and thermal conductivity detection (TCD), using helium as carrier gas.

Calculation of conversions and selectivity were carried out according to the general equations below:

Conversion of $x = C[x] =$ % conversion of x (including methane and oxygen) into all products

Yield of CO = $Y_{[CO]}$ = [amount of CO in products]/[amount of C in reactants]

Selectivity to CO = $S_{[CO]} = Y_{[CO]}/C_{[CH_4]}$

Yield of $H_2 = Y_{[H_2]} = 2$[amount of H_2 in products]/[amount of H in reactants]

Selectivity to $H_2 = S_{[H_2]} = Y_{[H_2]}/C_{[CH_4]}$

The deposited carbon was not taken into account. In all cases the carbon balances were better than 95%.

2.3. Catalyst characterizations

The crystalline components of the materials were identified by X-ray diffraction (XRD) using a D/max-RB model X-ray diffractometer with CuK_α radiation (λ = 0.15418 nm). The morphology of the passivated samples was observed using scanning electron microscopy (SEM) on a JSM-5600LV microscope. The BET specific surface areas of the passivated samples were measured on an ASAP 2010 (Micrometrics Instrument Corp.) using the N_2 adsorption method. Binding energy was determined by XPS using a spectrometer (ESCALAB 210) with monochromatic MgK_αexciting radiation (300 W, 30 eV), calibrated with C1s = 284.6 eV from contamination. Temperature programmed surface reaction (TPSR) with methane was carried out in AMI-100 catalyst characterization system (Altamira Instrument, USA). After the loaded sample (0.15 g) was pretreated with helium at 773 K for 0.5 h, it was heated at a ramped rate of 10 K min^{-1} from 473 to 1123 K in CH_4 atmosphere (30 ml min^{-1}). The desorbed products were determined by quadrupole mass spectrometry (Ametek Instruments, Dycor system 1000).

3. Results

3.1 Activity evaluation

The activity evaluation of catalyst for the POM to syngas is shown in Fig. 1 and Fig. 2. As shown in Fig. 1, the conversion of methane over 35.4 wt.% Mo_2C/Al_2O_3 catalyst decreased with time on stream from *ca.* 54% at the beginning to 44% in a period of 90 min under the reaction condition of T = 1123 K; GHSV = 20 500 ml h^{-1} g-Cat.$^{-1}$ and CH_4:O_2 = 2.05:1, while for the Mo_2C/Al_2O_3 catalyst doped with

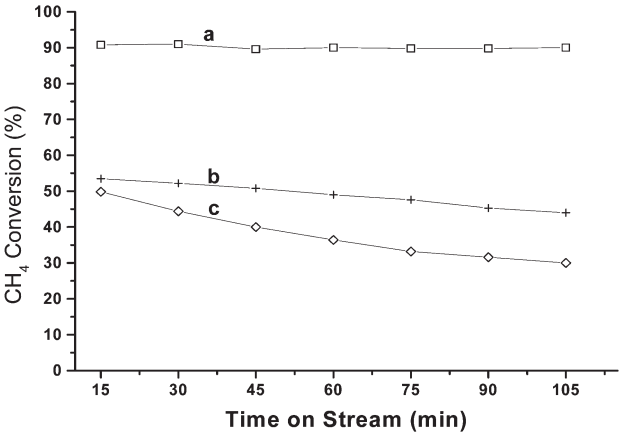

Fig. 1 Conversion of methane (%) *vs.* time on stream. (Reaction conditions: T = 1123 K; GHSV = 20 500 ml h^{-1} g-Cat.;$^{-1}$ CH_4:O_2 = 2.05:1. a, 0.5% Ni–35.4% Mo_2C/Al_2O_3; b, 35.4% Mo_2C/Al_2O_3; c, 0.5% Ni/Al_2O_3. mass ratio, same in the below.)

0.5 wt.% Ni, the conversion of methane was *ca.* 91%, almost constant with time on stream. As for 0.5 wt.% Ni/Al_2O_3 catalyst as a benchmark, the conversion of methane went down from *ca.* 50% at beginning to 30% in a period of 90 min. It is noted that the catalyst also underwent the same procedure, namely, carburization and pretreatment with H_2, before evaluation. As shown in Fig. 2, there was a much higher selectivity to CO or H_2 (*ca.* 96%, respectively) and more stability for the nickel-doped Mo_2C/Al_2O_3 catalyst than that for Mo_2C/Al_2O_3 catalyst.

It is well known that nickel is also highly active for the POM to syngas. In view of this, samples with more loading of nickel were not examined because it was difficult to distinguish the role of nickel from the carbide's.

3.2 Catalyst characterizations

The XRD patterns of the passivated carbide catalysts post-catalysis for 5 h are shown in Fig. 3. The presence of diffraction peaks at 2θ = 34.4, 38.0, 39.4, 61.5 and 69.6° indicated that molybdenum carbide doped with nickel or not existed in the form of β-Mo_2C according to refs.27 and 31. The diffraction peaks at 2θ = 26.1, 37.0, 37.4 and 52.2° showed the appearance of MoO_2 according to JCPDS 32-0671. However, there was almost no sign of the formation of MoO_2 for the nickel doped catalyst post-catalysis for 5 h. The peaks at 2θ = 45.1, 37.0 and 67.0° indicated that γ-Al_2O_3 had transformed into δ-Al_2O_3 (JCPDS 47-1770) after the reaction. As for the Ni/Al_2O_3 sample, no diffraction peak involved with nickel was

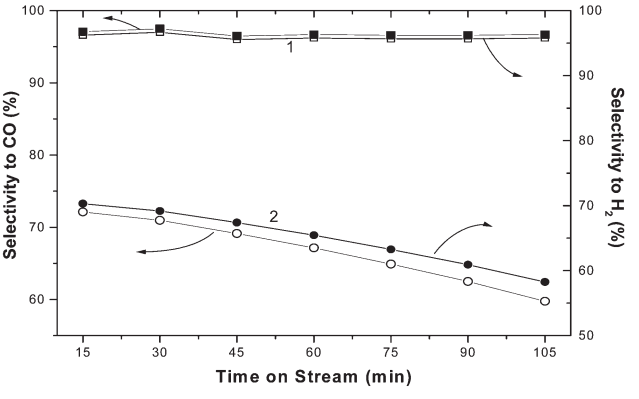

Fig. 2 Selectivity to CO or H_2 *vs.* time on stream. (Reaction conditions same as in Fig. 1: 1, 0.5% Ni–35.4% Mo_2C/Al_2O_3; 2, 35.4% Mo_2C/Al_2O_3.)

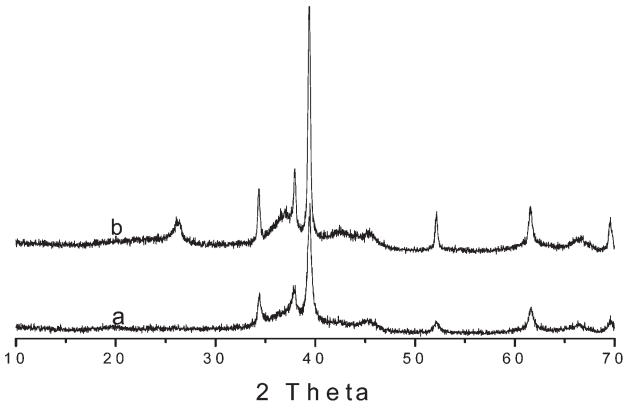

Fig. 3 XRD patterns of the passivated carbide catalysts post-catalysis for 5 h (a, 0.5% Ni–35.4% Mo_2C/Al_2O_3; b, 35.4% Mo_2C/Al_2O_3).

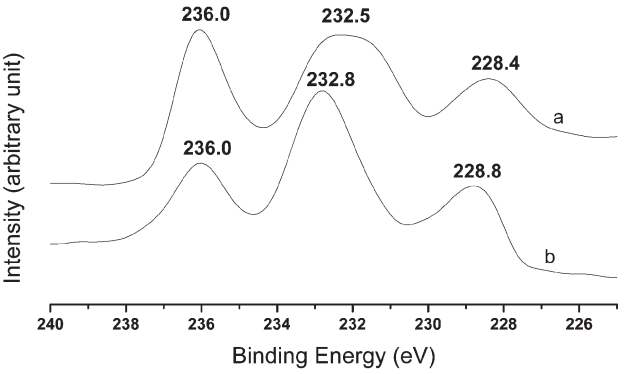

Fig. 5 Mo3d XPS spectra of passivated samples (a, 0.5% Ni–35.4% Mo_2C/Al_2O_3; b, 35.4% Mo_2C/Al_2O_3. post-catalysis for 5 h).

observed. There were two reasons for this: one was the high dispersion, and the other was low content, of nickel.

The BET surface areas for fresh samples were 100.4 and 101.3 for the undoped and the nickel doped sample, respectively, 65.9 and 89.5 $m^2\ g^{-1}$ for the undoped and the nickel doped sample post-catalysis for 5 h, respectively.

The scanning electron micrographs (Fig. 4) showed that there were smaller particles over the surface of the nickel doped sample, while there were larger particles of the undoped sample.

The XPS results are shown in Figs. 5, 6, 7 and 8. As shown in Fig. 5, the peak at 228.4 for the nickel doped, 228.8 eV for the undoped sample post-catalysis for 5 h was attributed to the binding energy of $Mo3d_{5/2}$ in carbide.[32,33] The peak at 236.0 was attributed to $Mo3d_{3/2}$ with high oxidation number, while the peak at 232.5 or 232.8 eV was attributed mixed peaks of $Mo3d_{5/2}$ with high oxidation number and $Mo3d_{3/2}$ from carbide.

The C1s XPS spectra are shown in Figs. 6 and 7. The carbidic C1s peak was not observed in any case. When the binding energy of Al2p in samples, 75.0 ~ 75.2 eV, was taken as a reference, it was also difficult to attribute any peak to the carbidic C1s peak. This phenomenon was also observed by Ding *et al.*.[34] It may stem from the carbidic carbon covered with a layer of deposited carbon. Thus, the main peak at 284.6 eV was ascribed to the C1s binding energy from the deposited carbon. As shown in Figs. 6 and 7, the C1s XPS spectra can be deconvoluted into three peaks. The main peak at 284.6 eV was attributed to the C1s from deposited carbon, the peak at 285.8 for the undoped, at 285.5 eV for the nickel doped sample, to the C–O species, the peak at 289.4 for the undoped, at 289.7 eV for the nickel doped, to the C=O species.[35,36]

O1s XPS spectra are shown in Fig. 8. The binding energy of O1s from carbide catalysts was higher than that from oxide, and it was higher for the nickel doped than that for the undoped sample.

Desorption of main products during CH_4-TPSR is shown in Figs. 9 and 10. The water (m/e = 18) desorption peaks occurred at 936 and 997 K for the undoped sample, at *ca.* 870 and 919 K for the nickel doped sample. The CO (m/e = 28) desorption formed a small peak at 862 K and a strong peak within temperature range from 960 to 1019 K for the undoped sample, a very small peak at 848 and a strong peak at 914 K for the nickel doped sample. CO_2 (m/e = 44) desorption formed a dune-like peak at 901 K and a peak 972 K for the undoped sample, a peak at 909 K for the nickel doped sample. H_2 formation at *ca.* 945 K for the undoped sample, at 909 K for the nickel doped sample came to such degree that it exceeded the detectable scope of the instrument.

4. Discussions

The results of Figs. 1 and 2 indicate that addition of nickel promotes the conversion of methane and selectivity to CO and H_2. From the catalytic performance at the initial stage, the stability was also improved. In fact, the methane conversion and the selectivity of products were hardly decreased after 16 h run (results are not given in this paper). Although nickel is very active for the POM to syngas, apparently, the conversion of methane shown in Fig. 1(a) is not the result of added nickel and also not the simple sum of that of 35.4% Mo_2C/Al_2O_3 (b) or that of 0.5% Ni/Al_2O_3 (c). This implied that the addition of

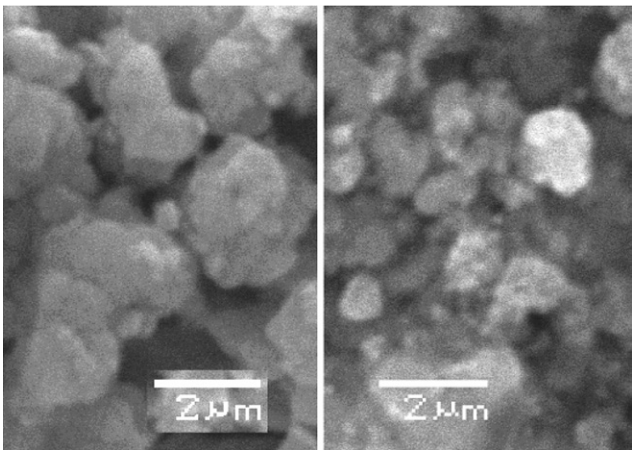

Fig. 4 Micrographs of samples post-catalysis for 5 h (left, 35.4% Mo_2C/Al_2O_3; right, 0.5% Ni–35.4% Mo_2C/Al_2O_3).

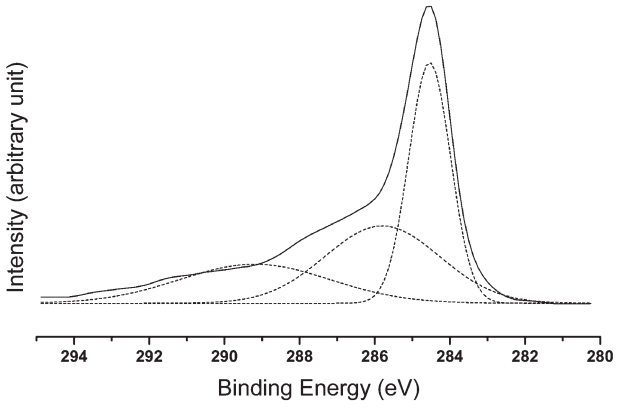

Fig. 6 C1s XPS spectra of passivated 35.4 wt.% Mo_2C/Al_2O_3 catalyst post-catalysis for 5 h.

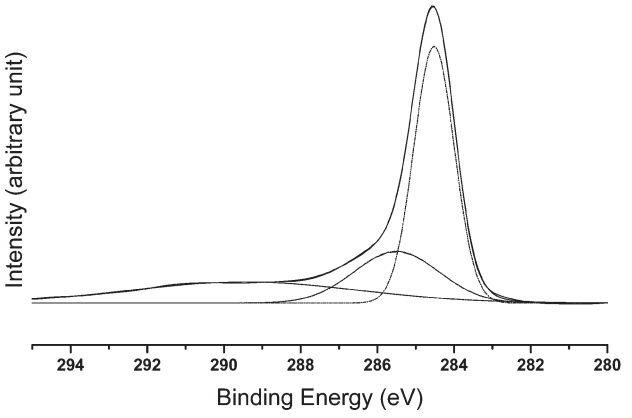

Fig. 7 C1s XPS spectra of passivated 0.5% Ni–35.4% Mo_2C/Al_2O_3 catalyst post-catalysis for 5 h.

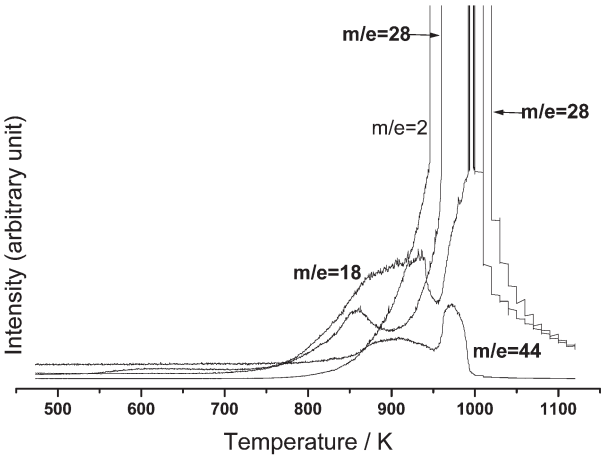

Fig. 9 Product desorption over 50% MoO_3/Al_2O_3 during CH_4-TPSR.

nickel resulted in a synergism between nickel and molybdenum carbide. As for the deactivation of the Mo_2C/Al_2O_3 catalyst, this was mainly due to the reasons described in ref. 27 while the Ni/Al_2O_3 catalyst may be mainly due to carbon deposition under the reaction conditions, $CH_4:O_2 > 2$.

Usually, molybdenum carbide obtained from its oxide or hydroxide carburized with the mixture of methane and hydrogen is β-Mo_2C (hcp).[27,31,32] As shown in Fig. 3, the main surface phases of catalyst, whether doped with nickel or not, were still β-Mo_2C, and were not affected, at least not significantly, by the nickel modification or its use in catalysis. However, for the nickel doped sample, there was no phase associated with nickel identified by XRD. Besides the low content of nickel and sensitivity of the diffractometer, the high dispersion of nickel should be also responsible for this. The obvious discrepancy between the undoped and the nickel doped sample post-catalysis was the MoO_2 formation. There was some MoO_2 formed over Mo_2C/Al_2O_3 post-catalysis for 5 h, but the MoO_2 phase was hardly formed for the nickel doped sample post-catalysis.

BET surface area is crucial to catalysis. As mentioned above, the surface area of the nickel doped sample was a little larger than that of the undoped sample. Although this margin fell in the error range, it was in agreement with the result of the specific surface area increasing with the elevated carburization degree.[31] As for this, it will be discussed later. After the catalysts were used for the POM to syngas, the surface area of the undoped catalyst decreased drastically, while the surface area of the nickel doped catalyst did relatively slowly. This decrease primarily resulted from the sintering of molybdenum species, including carbide and oxycarbide as well as oxide, during the reaction at high temperature. Among these species, molybdenum oxide was easily to sinter due to its relatively lower melting temperature. Judging by the difference of specific surface area between pre- and post-catalysis, the added nickel was able to resist sintering to some extent. From the Hüttig temperature, the nickel is not able to promote the resistance against the sintering due to its lower melting point than molybdenum metal.[37] This function of added nickel can be explained as follows: the added nickel promoted the transformation of oxide into carbide, while the carbide was difficult to sinter because it is of much higher melting point than that of the oxide. This function was also reflected in its morphology as shown in Fig. 4: the doped nickel resulted in smaller carbide particles over the surface, or else more and larger agglomeration occurred due to aggravated sintering. As for the promotion of nickel to the transformation of oxide into carbide, it will be discussed later on.

Mo3d XPS spectrum reveals that the added nickel led to the binding energy of carbide shifting to the lower end (Fig. 5). Although any oxidation state of Mo in carbide is possible,[32] it is difficult to determine the binding energy of each Mo species from Fig. 5. Even the peaks are deconvoluted, the obtained results will be affected by many factors. For the convenience of discussion, the oxidation states of Mo in Fig. 5 are divided into three kinds, high, medium and low oxidation state. It could be found that the binding energy of Mo with high oxidation state was not affected by the addition of nickel. This Mo species may originate from the passivation because the freshly carburized sample is very active for the oxidation

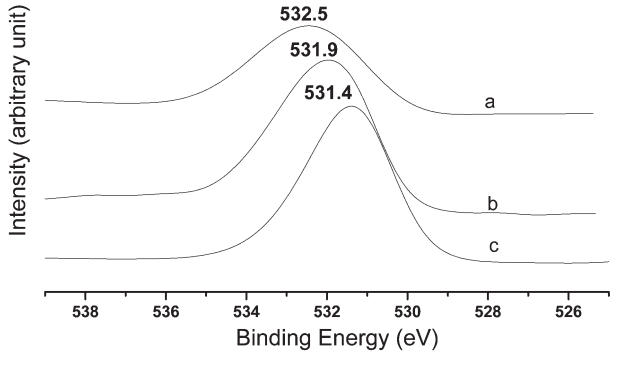

Fig. 8 O1s XPS spectra of samples (a, passivated 0.5% Ni–35.4% Mo_2C/Al_2O_3 catalyst post-catalysis for 5 h; b, passivated 35.4% Mo_2C/Al_2O_3 catalyst post-catalysis for 5 h; c, fresh 50% MoO_3/Al_2O_3).

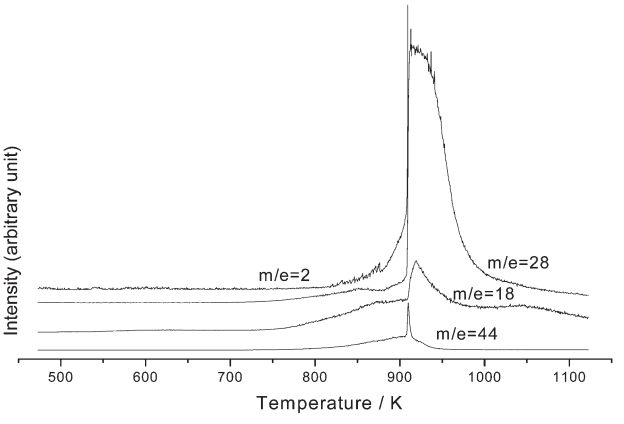

Fig. 10 Product desorption over 0.5% Ni–50%MoO_3/Al_2O_3 during CH_4-TPSR.

when contacted with air, which was described in many references. Also it possibly resulted from the oxidation during the POM to syngas. However, the binding energy of Mo with medium or low oxidation state, associated with carbide,[32,35] was shifted to the lower end. This shift was attributed to the difference of ligand layers around molybdenum ion, namely, carburization degree. The increase of C atoms as a ligand of Mo results in the binding energy shifting to the lower end because they lead to the d-orbital occupation increasing according to refs.38 and 39. This means C atoms play the equivalent role of electron donor. Contrary to C atoms, the increase of O atoms round Mo ion results in the binding energy shifting to higher end. Judging by these results, the addition of nickel favours the preservation of carbide during the POM to syngas.

As mentioned above, the C1s XPS spectra can be deconvoluted into three peaks which correspond to different species. Among them, the species containing C=O, such as absorbed CO_2 or surface carboxyl, corresponds to higher binding energy. The species containing C–O, usually formed *via* carbon atoms in carbide replaced by oxygen atoms, corresponds to medium binding energy, while the deposited carbon corresponds to lower binding energy. These are shown in Figs. 6 and 7. In addition to those mentioned above, there should be a kind of species, carbide carbon, whose binding energy of C1s should be lower than 284.6 eV (contaminated carbon).[33] However, it was not found in our experiment due to the possible reason mentioned above. As shown in Figs. 6 and 7, there were more species containing oxygen for the undoped sample than that of the nickel doped judging from the relative intensity. The introduction of oxygen may originate from the POM reaction or/and its passivation, even it was possible for a trace amount of oxygen left from the carburization. At all events, the result also manifested that the addition of nickel prevented the catalyst from oxidation.

The binding energy of O1s (Fig. 8) depends upon its coordinate situation. In other words, it is associated with its real oxidation state. The binding energy of O1s in carbide was higher than that in oxide, which was attributed to the electron donation of carbon atoms. Accordingly, that the binding energy of O1s in the nickel doped sample was higher than that in the undoped sample indicated that there were more carbon atoms around an oxygen atom in the nickel doped sample than that in the undoped sample, namely, there was higher carburization degree in the nickel doped than that in the undoped sample. This result draws the same conclusion: the addition of nickel is favourable to the maintenance of carbide during the POM to syngas.

The main products of MoO_3 reduced with CH_4 are CO, CO_2 and H_2O. Judging by the formation of these compounds during CH_4-TPSR over the supported oxide samples, the precursors of corresponding carbide catalysts, the addition of nickel was favourable to the reduction of MoO_3 with CH_4 (compare Figs. 9 and 10) because these products were formed at a lower temperature over the nickel doped sample. With the increasing temperature, the oxygen atoms in oxide were continuously removed, which led to O atom vacancies left. On the other hand, H or C atoms resulting from the dissociation of methane could possibly occupy these vacancies, and this possibility increased with temperature. When a portion of oxygen was replaced by carbon atoms, oxycarbide was formed,[35] and this replacement resulted in the formation of carbide in the end.[33] According to these viewpoints, the addition of nickel was also favourable to the carburization of molybdenum oxide. This function of nickel was similar to that of cobalt.[40] If so, there was greater degree of carburization for the nickel doped sample at the same temperature. In the course of carburization, the replacement of oxygen atoms by carbon atoms will result in the expansion of crystal lattice,[38,39] which further results in a larger specific area.[31] In fact, the results of BET surface area mentioned above supported this conclusion.

However, H_2 was formed at temperatures at which methane cannot be pyrolyzed under normal conditions, in the course of CH_4-TPSR. Therefore, the formation of hydrogen resulted from the catalytic decomposition. It can be found from Figs. 9 or 10 that the initial formation of hydrogen occurred at higher temperatures than that of CO or CO_2. This indicated that the catalysis cannot come from the catalysis of the MoO_3 phases. From the H_2 formation *vs.* temperature as shown in Figs. 9 and 10, it could be conjectured that oxycarbide or carbide can catalyze the decomposition of methane, especially the oxycarbide, no matter at what temperature oxycarbide was to be formed. The activation of methane is the precondition of methane decomposition. In comparison with Fig. 9, H_2 formation (same intensity) occurred at a lower temperature (Fig. 10). This showed that the nickel doped sample had greater ability to activate methane. This promotion of nickel comes from aspects, such as active centers per unit area and the intrinsic activity of catalytic center *etc.* The coordinately unsaturated sites (CUS) in carbide are usually regarded as active centers.[41] CUS as surface defects are usually located at edges, fissures, steps *etc.* They can be formed *via* routes, but mainly result from the carburization. When the carbon atoms diffuse into the bulk oxide or oxycarbide in the course of carburization, a portion of particles is split into smaller particles due to the difference of atom size between C and O; meanwhile, the crystal lattice is expanded. This cleavage of particles is speeded up with increased temperature or carburization. This means the carburization degree results in the increase of surface density of active centers. The effect of carburization degree on catalytic performance is as Choi *et al.* said: 'the higher degree of carburization, the more noble metal-like behaviours'.[42] According to the essential interpretation of the carbide catalysis,[38,39] the d-orbital occupation of Mo atom is crucial to its catalysis. If there is higher d-orbital occupation, there is greater catalysis. Nickel is usually used as an electron donor promoter, thus, the addition of nickel increases the d-orbital occupation of Mo atom, which results in higher intrinsic activity of molybdenum carbide.

The promotion of nickel to the carburization of molybdenum oxide, in particular under the condition of the POM to syngas, is important. It can make more carbide or oxycarbide phases be preserved, while the carbide or oxycarbide are highly active phases. At same time, the promotion of nickel can elevate the carburization degree, which means that the active phases have a higher density of active centers and higher intrinsic activity as well as greater ability to resist sintering. In addition, the higher carburization degree can also result in stable catalytic performance owing to the reasons mentioned above. Although only the improvement of stability at initial reaction stage is given, it is reasonable to predict that the addition of nickel is favourable to improving the stability of catalytic performance. Therefore, the nickel doped carbide catalyst can be expected to exhibit higher activity, higher selectivity and higher catalytic stability for the POM to syngas.

Molybdenum carbide is active for the POM, but it is easily to deactivate mainly due to its transformation into oxide. Nickel is active for the POM, but it also catalyzes the formation of deposited carbon. It is possible for the catalyst based upon molybdenum carbide and nickel to eliminate the above shortcoming. This is very significant for the POM to syngas.

5. Conclusions

The added nickel showed excellent promotion to molybdenum carbide catalyst for the POM to syngas. This mainly includes promotion of the reduction of molybdenum oxide, and thus further to the carburization, which results in a higher degree of carburization under the same conditions. Under the conditions of the POM to syngas, this promotion leads to more

carbide or oxycarbide phases, active phases which have higher density of active sites and higher intrinsic activity for the activation of methane, being held. Also the carbide catalyst is of larger specific area and greater ability to resist sintering when it is of higher degree of carburization. Of course, nickel itself also makes a rather contribution to the POM to syngas.

Acknowledgements

This work has been financially supported by the Foundation of National Fundamental Research & Development.

References

1 S. T. Oyama, *The Chemistry of Transition Metal Carbides and Nitrides*, ed. S. T. Oyama, Blackie Academic and Professional, Glasgow, 1996, p. 1.
2 E. K. Storms, *The Refractory Carbides*, Academic Press, New York, 1967.
3 L. E. Toth, *Transition Metal Carbides and Nitrides*, Academic Press, New York, 1971.
4 J. Luthin and C. Linsmeier, *J. Nucl. Mater.*, 2001, **290–293**, 121.
5 R. B. Levy and M. Boudart, *Science*, 1973, **181**, 547.
6 J. C. Schlatter, S. T. Oyama, J. E. Metcalfe III and J. M. Lambert, Jr, *Ind. Eng. Chem. Res.*, 1988, **27**, 1648.
7 J. G. Choi, J. R. Brenner and L. T. Thompson, *J. Catal.*, 1995, **154**, 33.
8 J. S. Lee and M. Boudart, *Appl. Catal.*, 1985, **19**, 207.
9 E. J. Markel and J. W. Van Zee, *J. Catal.*, 1990, **126**, 643.
10 D. J. Sajkowski and S. T. Oyama, *Appl. Catal. A*, 1996, **134**, 339.
11 C. W. Colling, J. G. Choi and L. T. Thompson, *J. Catal.*, 1996, **160**, 35.
12 G. M. Dolce, P. E. Savage and L. T. Thompson, *Energy Fuels*, 1997, **11**, 3.
13 Y. Zhang, Z. Wei, W. Yan, P. Ying, C. Ji, X. Li, Z. Zhou, X. Sun and Q. Xin, *Catal. Today*, 1996, **30**, 135.
14 C. Sayag, S. Suppan, J. Trawczynski and G. Djéga-Mariadassou, *Fuel Process. Technol.*, 2002, **77–78**, 261.
15 T. C. Xiao, A. P. E. York, H. Al-Megren, J. B. Claridge, H. T. Wang and M. L. H. Green, *C. R. Acad. Sci., Ser. IIc: Chim.*, 2000, **3**, 451.
16 E. Iglesia, F. H. Riberio, M. Boudart and J. E. Baumgartner, *Catal. Today*, 1992, **15**, 307.
17 E. Iglesia, F. H. Riberio, M. Boudart and J. E. Baumgartner, *Catal. Today*, 1992, **15**, 455.
18 E. A. Blekkan, C. Pham-Huu, M. J. Ledoux and J. Guille, *Ind. Eng. Chem. Res.*, 1994, **33**, 1657.
19 C. Pham-Huu, M. J. Ledoux and J. Guille, *J. Catal.*, 1993, **143**, 249.
20 C. Pham-Huu, A. P. E. York, M. Benaissa, P. Del Gallo and M. J. Ledoux, *Ind. Eng. Chem. Res.*, 1995, **34**, 1107.
21 K. Y. Park, W. K. Seo and J. S. Lee, *Catal. Lett.*, 1991, **11**, 349.
22 H. C. Woo, K. Y. Park, Y. G.. Kim, I. S. Nam, J. S. Chung and J. S. Lee, *Appl. Catal. A*, 1991, **75**, 267.
23 M. Nagai, T. Kurakami and S. Omi, *Catal. Today*, 1998, **45**, 235.
24 R. Miles, *J. Chem. Technol. Biotechnol.*, 1980, **30**, 35.
25 N. Nakazawa and H. Okamoto, *Appl. Surf. Sci.*, 1985, **24**, 75.
26 A. P. E. York, J. B. Claridge, A. J. Brungs, S. C. Tsang and M. L. H. Green, *Chem. Commun.*, 1997, 39.
27 J. B. Claridge, A. P. E. York, A. J. Brungs, C. Marquez-Alvarez, J. Sloan, S. C. Tsang and M. L. H. Green, *J. Catal.*, 1998, **180**, 85.
28 A. P. E. York, J. B. Claridge, A. J. Brungs, C. Márquez-Alvarez, S. C. Tsang and M. L. H. Green, *Stud. Surf. Sci. Catal.*, 1997, **110**, 711.
29 L. Volpe and M. Boudart, *J. Solid State Chem.*, 1985, **59**, 332.
30 L. Volpe and M. Boudart, *J. Solid State Chem.*, 1985, **59**, 348.
31 A. Hanif, T. Xiao, A. P. E. York, J. Sloan and M. L. H. Green, *Chem. Mater.*, 2002, **14**, 1009.
32 K. Oshikawa, M. Nagai and S. Omi, *J. Phys. Chem. B*, 2001, **105**, 9124.
33 L. Leclercq, M. Provost, H. Pastor, J. Grimblot, A. M. Hardy, L. Gengembre and G. Leclercq, *J. Catal.*, 1998, **117**, 371.
34 Z. Ding, S. Sheng, J. Zhu, X. Zhu, G. Xiong and S. Zhuangm, *Chin. J. Chem. Phys.*, 1997, **10**, 237.
35 P. Delporte, F. Meunier, C. Pham-Huu, P. Vennegues, M. J. Ledoux and J. Guille, *Catal. Today*, 1995, **23**, 251.
36 M. Bou, J. M. Martin, T. LcMognc and L. Vovelle, *Appl. Surf. Sci.*, 1991, **47**, 149.
37 M. S. Spencer, *Nature*, 1985, **323**, 685.
38 R. Siegel, *Semicond. Insul.*, 1979, **5**, 47.
39 V. Heine, *Phys. Rev.*, 1967, **153**, 673.
40 T. C. Xiao, A. P. E. York, H. Al-Megren, C. V. Williams, H. Tao Wang and M. L. H. Green, *J. Catal.*, 2001, **202**, 100.
41 P. A. Aegerter, W. W. C. Quigley, G. J. Simpson, D. D. Ziegler, J. W. Logan, K. R. McCrea, S. Glazier and M. E. Bussell, *J. Catal.*, 1996, **164**, 109.
42 J. S. Choi, G. Bugli and G. Djéga-Mariadassou, *J. Catal.*, 2000, **193**, 238.